Pharmaceutical Research, Vol. 26, No. 2, February 2009 (© 2008)
DOI: 10.1007/s11095-008-9757-2

Research Paper

Effect of Diabetes on Transscleral Delivery of Celecoxib

Narayan P. S. Cheruvu,[1,3] Aniruddha C. Amrite,[1,4] and Uday B. Kompella[1,2,5]

Received July 14, 2008; accepted October 10, 2008; published online November 6, 2008

Purpose. To investigate the effects of diabetes on transscleral retinal delivery of celecoxib in albino and pigmented rats.
Methods. Albino (Sprague Dawley—SD) and pigmented (Brown Norway—BN) rats were made diabetic by a single intraperitoneal injection of streptozotocin (60 mg/kg) following 24 h of fasting and diabetes was confirmed (blood glucose >250 mg/dL). Two months after diabetes induction, the integrity of blood-retinal-barrier in control *versus* diabetic rats from both strains was compared by using FITC-dextran leakage assay. Fifty microliter suspension of celecoxib (3 mg/rat) was injected periocularly in both the strains in one eye, 2 months following diabetes induction. The animals were euthanized at the end of 0.25, 0.5, 1, 2, 3, 4, 8, and 12 h post-dosing and celecoxib levels in ocular tissues and plasma were estimated using a HPLC assay.
Results. Diabetes (2-month duration) resulted in 2.4 and 3.5 fold higher blood-retinal barrier leakage in diabetic SD and BN rats, respectively, compared to controls. The area under tissue celecoxib concentration *versus* time curves (AUC) for sclera, cornea, and lens were not significantly different between control and diabetic animals. However, retinal and vitreal AUCs of celecoxib in treated eyes were approximately 1.5-fold and 2-fold higher in diabetic SD and BN rats, respectively, as compared to the controls.
Conclusions. Transscleral retinal and vitreal delivery of celecoxib is significantly higher in diabetic animals of both strains. The increase in retinal delivery of celecoxib due to diabetes is higher in pigmented rats compared to albino rats. Higher delivery of celecoxib in diabetic animals compared to control animals can be attributed to the disruption of blood-retinal barrier due to diabetes.

KEY WORDS: blood-retinal-barrier; diabetes; periocular injection; pigmentation; transscleral.

INTRODUCTION

Among the various eye diseases, diabetic retinopathy and age related macular degeneration (ARMD) account for ~40% vision loss or blindness in adults 40 years or older (1). Traditional approaches in treating these diseases (e.g., laser treatment and photodynamic therapy) delay vision loss by controlled damage to the affected region of the retina but they do not improve or reverse vision loss (2). Recent understanding of the pathophysiological conditions of these diseases has led to the development of various drugs including Lucentis®, which not only prevents vision loss in ARMD but also helps in vision gain (2). Further, various experimental small molecule therapeutics like anecortave acetate (3), budesonide (4), and celecoxib (5) have shown promising results in alleviating diabetic retinopathy conditions in animal models. However, delivery of most of these drugs by systemic mode of administration is limited due to various physiological barriers like the inner-blood-retinal barrier, outer blood retinal barrier and dose limiting systemic side effects. Intravitreal injections and implants (conventional modes of drug delivery to the retina) are associated with side effects such as retinal damage and ocular infection. Previous studies from our group (6) and others (7,8) have shown that transscleral drug delivery using periocular (e.g., subconjunctival and sub-tenon) injections is a viable alternative in localized drug delivery to the retina.

Sclera, with its larger surface area (about 95% of total eye surface), hypocellular nature, ease of access (9), and high permeability characteristics is shown to be a promising route for delivery for both small (10) and high (11) molecular weight drugs to the retina. The role of various parameters like age of sclera (12), intra-ocular pressure (13), scleral thickness (14), scleral hydration (15), choroidal blood flow (16), lymphatic uptake (16), and retinal pigment epithelium (17) on retinal drug delivery by transscleral route has been previously reported. We have reported that the pigmented nature of choroid and its affinity for lipophilic solutes reduces transscleral transport of lipophilic molecules (e.g., celecoxib) more compared to hydrophilic solutes (18). Pigmentation also decreases transscleral delivery of molecules like celecoxib *in vivo* (19).

When a drug is injected by periocular injection, a bleb is formed at the site of administration, which dissipates over time. The drug would be either absorbed transsclerally to be delivered to the retina or eliminated from the site of administration through the periocular and conjunctival blood

[1] University of Nebraska Medical Center, Omaha, Nebraska 68198-6025, USA.
[2] Departments of Pharmaceutical Sciences and Ophthalmology, University of Colorado Denver, Aurora, Colorado 80045, USA.
[3] *Present address:* Covidien Ltd., Hazelwood, Missouri, USA.
[4] *Present address:* Quintiles Inc., Overland Park, Kansas, USA.
[5] To whom correspondence should be addressed. (e-mail: Uday.Kompella@uchsc.edu)

Table I. Body Weights and Blood Sugar Levels in Study Groups

Strain	Group	Blood glucose levels (mg/dL)	Weight (gm)
SD	Control	129 ± 12	225 ± 10
SD	Diabetic	426 ± 24	218 ± 24
BN	Control	133 ± 16	230 ± 15
BN	Diabetic	430 ± 33	220 ± 29

Blood glucose levels and weights for control and diabetic animals were measured on day 1 and on day 60, respectively. The data are expressed as mean±SD

and lymphatic systems. Based on the experimental data obtained using rat models, we developed and validated a pharmacokinetic compartmental model to understand the drug disposition following periocular injection (20). Based on this model in Brown Norway rats, the drug dissolution/release rate constant for celecoxib in the periocular space was found to be 0.017 min^{-1}. The absorption rate constant into sclera and choroid–RPE was found to be 3.61×10^{-4} min^{-1} and the drug elimination rate form the periocular site of administration was estimated to be 0.12 min^{-1}. Thus, transscleral drug delivery is limited by multiple barriers. From the studies done so far by various groups, the factors influencing transscleral drug delivery can be grouped into (i) physico-chemical parameters related to the drug and (ii) physiological parameters related to the surrounding tissue. However, there are no reports indicating the role of disease, e.g., diabetes, on transscleral drug delivery.

The effect of disease state, particularly ocular infections like endophthalmitis on ocular pharmacokinetics following topical and systemic delivery has extensively been investigated by Bozkurt's group (21–27). Results from their studies in humans and animal models indicate that inflammation in the eye can cause increased aqueous and vitreous levels of antibiotics following topical and systemic delivery. One of the possible reasons speculated for the increased aqueous and vitreous levels is the alteration in blood-retinal and blood-aqueous barriers. In another study, Blair *et al.* (28) have shown that the induction of diabetes in rats leads to diabetic retinal pigment epitheliopathy, one of the early changes of diabetic retinopathy, and increased permeability of systemically administered horseradish peroxidase. Zhang *et al.* (29) have reported genetic differences in the blood-retinal barrier breakage in Sprague Dawley and Brown Norway rats following streptozotocin induced diabetes. However, the effect of diabetes and the resulting breakdown of blood-retinal barrier on transscleral delivery have not been investigated. To this end, we investigated the effect of diabetes on the transscleral delivery of celecoxib in the current study. Celecoxib is a drug effective in alleviating the biochemical changes associated with diabetic retinopathy (5) and choroidal neovascularization (30) in a rat model. To account for the differences in pigmentation and the blood-retinal barrier breakdown between strains, we have investigated the difference in ocular pharmacokinetics using diabetic albino (Sprague Dawley) and pigmented (Brown Norway) rats.

MATERIALS AND METHODS

Chemicals

Celecoxib was purchased from Chempacific (Baltimore, MD, USA). Sodium salt of carboxy methyl cellulose (CMC; cat. no. C5678; viscosity: 50–200cps for 4% *w/v* aqueous solution at 25°C), budesonide, 4.4kDa FITC-Dextran and HPLC grade methylene chloride, glacial acetic acid and acetonitrile were purchased from Sigma Chemicals (St. Louis, MO). Pentobarbital sodium was purchased from Fort Dodge Laboratories (Fort Dodge City, IA, USA).

Animal Studies

All animals were treated according to the ARVO statement for the use of animals in ophthalmic and vision research. Male Sprague-Dawley (SD; albino) and male Brown-Norway (BN; pigmented) rats (SASCO) weighing 200–250 g were used in this study. Data for the control albino (SD) and pigmented (BN) rats was obtained from our previous study (19). Although it is easier to isolate eye tissues from a rabbit model, we used rat models for the following reasons. Rabbit retinal structure differs from the humans in terms of the microvasculature of the retina. The rabbits lack circulation in the inner retina (merangiotic retina) whereas humans and rats have an euangiotic retina (circulation present in the outer and inner retinal layers) (31). The rat retina is therefore anatomically similar to the human retina as compared to the rabbits. Also we were interested in studying the progression of diabetic retinopathy in the long term and no good model for diabetic retinopathy in rabbits exists. On the other hand, rat models for diabetic retinal complications are extensively utilized (32–40). In addition, publications from our group and other groups have shown that the biochemical changes in retina following induction of diabetes are similar to those observed in human retina (6,32–43).

Induction of Diabetes

Induction of diabetes in rats was achieved using a previously reported method (5). Briefly, both SD and BN

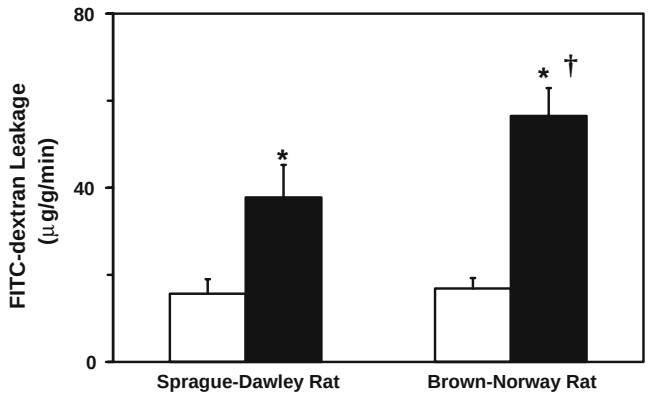

Fig. 1. Influence of diabetes on Sprague Dawley and Brown Norway rat blood-retinal-barrier leakage in normal (*open square*) and diabetic rats at the end of 2 months. * Significantly (P=0.004) different from control rats. *Single dagger* Significantly different (P=0.05) from SD rats. Data are presented as mean±s.d. for n=4.

Table II. Influence of Diabetes on the Plasma Pharmacokinetic Parameters of Celecoxib in Sprague-Dawley and Brown-Norway Rats Following Periocular Injection of Celecoxib Suspension to One Eye at a Dose of 3 mg/rat

	Sprague Dawley rats		Brown Norway rats	
	Control[a]	Diabetic	Control[a]	Diabetic
T_{max} (h)	1.52±0.61	1.62±0.29	1.68±0.24	1.34±0.55
C_{max} (ng/ml)	425.24±97.26	431.28±56.54	480.22±21.11	450.88±36.79
$t_{1/2}$ (h)	5.62±0.43	5.34±0.35	5.43±0.51	4.97±0.45
$AUC_{0-\infty}$ (ng.h/ml)	2,911±358	3,458±542	3,124±435	3,317±433
V_d/F (ml)	6,740±1,615	6,524±971	6,327±1,512	7,022±254
Cl/F (ml/h)	1,043±129	958±125	1,127±148	1,022±204

The data are expressed as mean±s.d. for $n=4$

[a] The tissue concentrations for all control rats were taken from Cheruvu *et al.* (19), with permission from the Association for Research in Vision and Ophthalmology

rats were administered with a single intraperitoneal dose of streptozotocin (60 mg/kg) prepared in 10 mM citrate buffer after fasting animals for 24 h. The blood glucose levels were measured using a glucometer (OneTouch Ultra, LifeScan, Milpitas, CA) 24 h after the administration of streptozotocin. The animals with blood glucose >250 mg/dl were deemed diabetic. Following the treatment, the animals were given free access to food and water for 2 months.

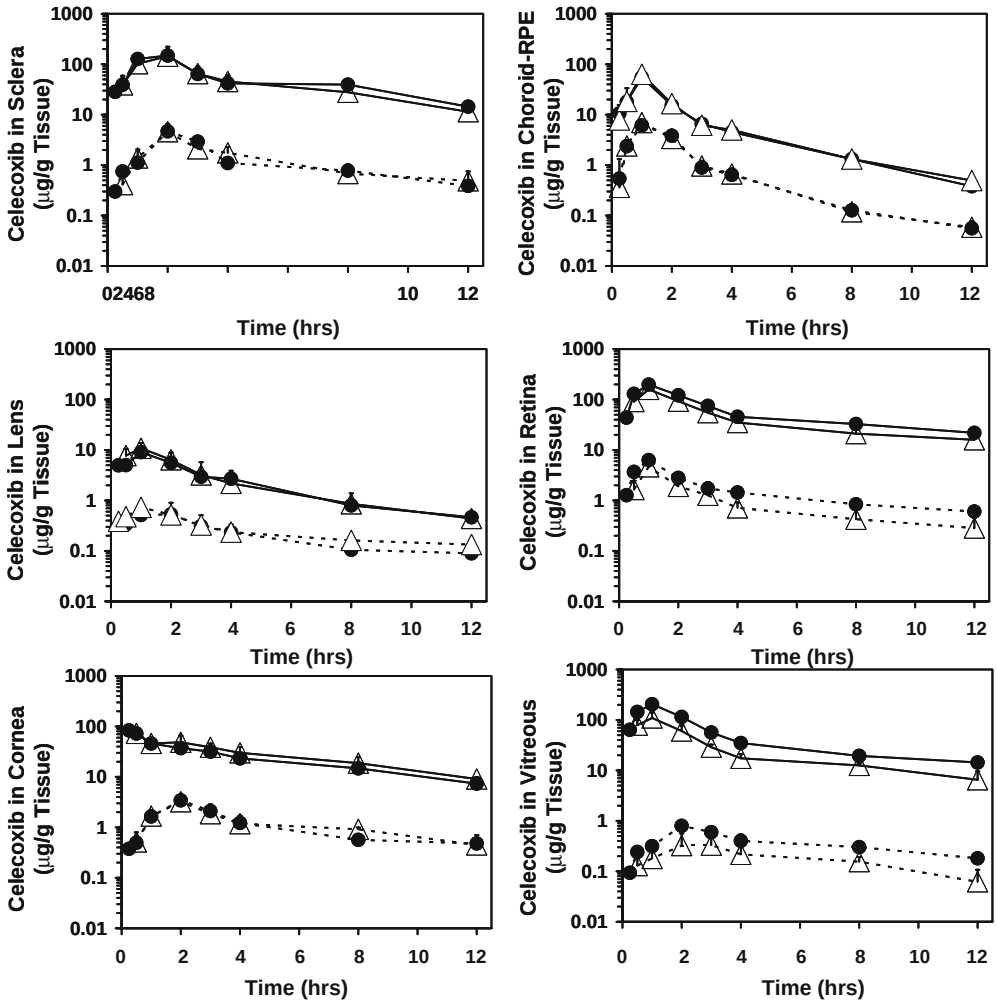

Fig. 2. Influence of diabetes on celecoxib delivery following periocular injection in (*open triangle*) control and (*closed circle*) diabetic Sprague Dawley rats. Key: *Continuous line* represents the ipsilateral eye and *broken line* represents the contralateral eye. Data are presented as mean±s.d. for $n=4$. The tissue concentrations for all control rats were taken from Cheruvu *et al.* (19), with permission from the Association for Research in Vision and Ophthalmology.

Blood-Retinal Barrier Leakage

The blood-retinal barrier leakage at the end of 2 months in both SD and BN rats was determined using FITC-dextran leakage assay, using previously reported method, with some modifications (44). Briefly, after induction of deep anesthesia, the animals were injected intravenously with FITC-dextran (4.4 kDa, 50 mg/mL in PBS, 50 mg/kg body weight). After 10 min, the chest cavity was opened, and the animals were perfused with PBS (500 mL/kg body weight) to remove the FITC-dextran remaining in the blood vessels. This perfusion removes the tracer trapped in the blood vessels, thereby allowing us to quantity only the tracer that leaked from the blood vessels into the retinal tissue. Blood samples were collected immediately before perfusion. Immediately after perfusion, the retinas were dissected and homogenized, and the FITC-dextran was extracted with 750 μL of water. The extract was centrifuged at 7,000 rpm for 10 min, and the supernatant (500 μL) was used to measure the fluorescence. Corrections for the blank were made by subtracting the fluorescence obtained from eyes of rats not injected with FITC-dextran. The amount of FITC-dextran in the samples was quantified using a standard curve of FITC-dextran in water. The amount of FITC-dextran in the retina was normalized to the retinal weight and to the plasma concentration of FITC-dextran. The blood-retinal barrier breakdown was calculated by using the following formula (44):

$$\frac{\text{Retinal FITC-dextran } (\mu g)/\text{retinal weight (g)}}{\text{Plasma FITC-dextran } (\mu g/\mu L) \times \text{circulation time (min)}}$$

Periocular Administration

At the end of 2 months following the induction of diabetes, periocular administration of celecoxib suspension was performed similar to previously reported method (45). Celecoxib was suspended (60 mg/ml) in 0.5% *w/v* of CMC in phosphate buffered saline (pH 7.4). The rats were anesthetized with an intraperitoneal injection of sodium pentobarbital (40 mg/kg) and (50 μl) of drug suspension was administered into the posterior subconjunctival space of one eye (ipsilateral) using a 27-gauge needle. The other eye (contralateral) served as a control. The animals were allowed to recover from anesthesia and water and food were provided *ad libitum* until euthanization. The animals were euthanized at 0.25, 0.5, 1, 2, 3, 4, 8, and 12 h post-dosing with sodium pentobarbital (250 mg/kg, i.p.). Blood samples were collected immediately after euthanization by cardiac puncture and

Table III. Influence of Diabetes on Ocular Tissue Pharmacokinetic Parameters of Celecoxib in Sprague Dawley Rats after Periocular Injection of Celecoxib Suspension to One Eye at a Dose of 3 mg/rat

Tissue	Condition	T_{max} (h)	C_{max} (μg/g tissue)	$T_{1/2}$ (h)	$AUC_{0-\alpha}$ (μg. h/g of tissue)	Cl/F (g/h)	V_d/F (g tissue)
Ipsilateral eye							
Sclera	Control	1.90±0.58	176.39±41. 22	6.10±1.30	860.05±57.99	4.78±0.59	27.03±6.02
	Diabetic	2.00±0.25	180.24±32.55	5.97±1.21	885.24±68.44	4.92±0.49	24.11±5.24
choroid–RPE	Control	1.00±0.00	55.14±15.64	2.40±0.10	252.27±34.58	33.15±5.5	115.33±24.30
	Diabetic	1.00±0.00	63.03±12.24	2.25±0.77	249.57±12.04	30.27±7.7	120.42±20.78
Retina	Control	1.25±0.50	159.79±32.12	5.99±2.38	670.94±103.69	4.60±0.71	38.31±11.24
	Diabetic	1.25±0.51	208.73±19.18*	6.06±0.96	1,059.33±125.78*	3.50±0.82	30.34±3.17
Vitreous	Control	0.88±0.25	116.34±24.90	5.5±1.70	368.40±52.14	8.31±1.22	56.24±14.25
	Diabetic	0.80±0.25	205.35±29.86*	5.19±1.74	576.50±143.89*	40.38±3.05*	189.02±40.60*
Lens	Control	1.00±0.08	10.87±2.89	8.71±3.03	185.94±48.05	93.21±28.33	720.12±617.24
	Diabetic	1.57±0.11	9.74±1.91	7.97±1.35	180.67±31.22	101.17±21.11	717.54±341.17
Cornea	Control	0.88±0.75	78.88±11.31	9.64±0.62	936.38±102.90	7.81±0.67	53.25±11.24
	Diabetic	0.79±0.21	75.23±12.10	9.12±0.75	942.55±90.21	6.91±0.52	50.17±9.91
Contralateral eye							
Sclera	Control	2.00±0.00	4.59±1.94	5.2±2.20	19.44±3.98	162.21±33.12	932.12±123.11
	Diabetic	2.00±0.00	4.22±1.07	5.88±1.21	18.36±2.64	159.22±30.57	1,077.64±97.48
choroid–RPE	Control	1.00±0.00	6.99±0.86	2.15±0.10	21.33±0.86	244.2±16.87	757.35±68.99
	Diabetic	1.00±0.00	5.87±0.59	2.53±0.31	22.42±0.95	238.5±21.27	832.13±73.25
Retina	Control	1.88±0.80	4.65±2.74	4.70±1.93	13.80±3.92	232.21±63.25	1,294±507.21
	Diabetic	2.00±0.40	6.32±0.35*	6.28±1.78	18.42±0.58*	125.10±23.24*	1,127±290.68
Vitreous	Control	2.75±0.96	0.53±0.30	7.10±2.66	2.80±1.13	1,161.21±320.98	9,392±3,535
	Diabetic	2.50±0.5	0.80±0.07*	5.19±0.67	3.50±0.15	1,264.22±111.18	15,233±1,978
Lens	Control	1.38±0.75	0.75±0.19	7.70±2.31	0.59±0.19	1,101.22±308.21	11,296±1,855
	Diabetic	1.50±0.87	0.79±0.11	7.13±1.97	0.55±0.08	1,097.11±256.11	11,321±1,752
Cornea	Control	2.00±0.00	3.41±0.32	7.21±2.05	0.65±0.33	197.78±79.34	1,239.25±136.97
	Diabetic	2.00±0.00	3.22±0.57	6.99±1.97	0.67±0.19	200.22±39.28	1,973.12±149.17

The data are expressed as mean±SD for n=4. The tissue concentrations for all control rats were taken from Cheruvu *et al.* (19), with permission from the Association for Research in Vision and Ophthalmology. C_{max}, Cl/F, and V_d/F values in ipsilateral eye were significantly (p=0.0001) different compared with the contralateral eye in all groups

*P<0.05 (significant difference compared to the corresponding control SD rat tissues)

the eyes were enucleated and frozen at −80°C. The ocular tissues including the sclera, choroid–RPE, retina, vitreous, lens, and cornea were isolated. Isolation of the ocular tissues was achieved using the following procedure. Empty eppendorf tubes (1.0 ml) were maintained at freezing temperatures by dipping them in dry ice and ethanol mixture before enucleating the eyes from animals. Immediately following the enucelation, the eyes were collected into the above tubes. The eyes were stored at −80°C prior to analysis. To minimize the redistribution of the drug during isolation, the following procedure was adopted. Isolation of the ocular tissues in cold conditions was achieved using a cooled dissection blade (kept at −80°C) and using a porcelain platform cooled using dry ice. Isolation of the individual tissues was achieved by observing the eye under dissection microscope. The eye was cut along the limbus area to isolate the anterior tissues: cornea and the lens. From the posterior section of the eye, vitreous (solidified) was collected. The retina and choroid–RPE were gently peeled from the adherent sclera using the dissection microscope. The ocular tissues were weighed and the celecoxib concentration was estimated using a previously reported HPLC assay (6).

HPLC Analysis of Celecoxib

Plasma and ocular tissue celecoxib levels were estimated as described previously (45). Briefly, the isolated ocular tissues were homogenized using 200 µl of PBS buffer and a Tissue Tearer (Biospec Products, Racine, WI, USA). To 200 µl of plasma or tissue homogenate, 5 µl of 40 µg/ml of budesonide was added as an internal standard and mixed thoroughly. Methylene chloride (2 ml) was added to the contents and mixed thoroughly for 15 min using a vortex mixer (Scientific Industries, Inc., Bohemia, NY, USA). The organic layer was separated and evaporated (N-evap Organomation, Berlin, MA, USA). The residue was reconstituted in 200 µl of mobile phase, centrifuged for 10 min at 12,000 × *g*, and 100 µl of the supernatant was injected onto Waters HPLC system that included a pump (Waters TM 616, Milford, MA), a controller (Waters 600S), an autoinjector (Waters 717 plus), and a PDA detector (Waters 996) set at a range of 190–400 nm. The drugs were separated using a 25 × 5 mm Discovery C-18 column (Supelco, Emeryville, CA, USA) with a particle diameter of 5µm and a pore size of 100 Å. The mobile phase for the assay consisted of

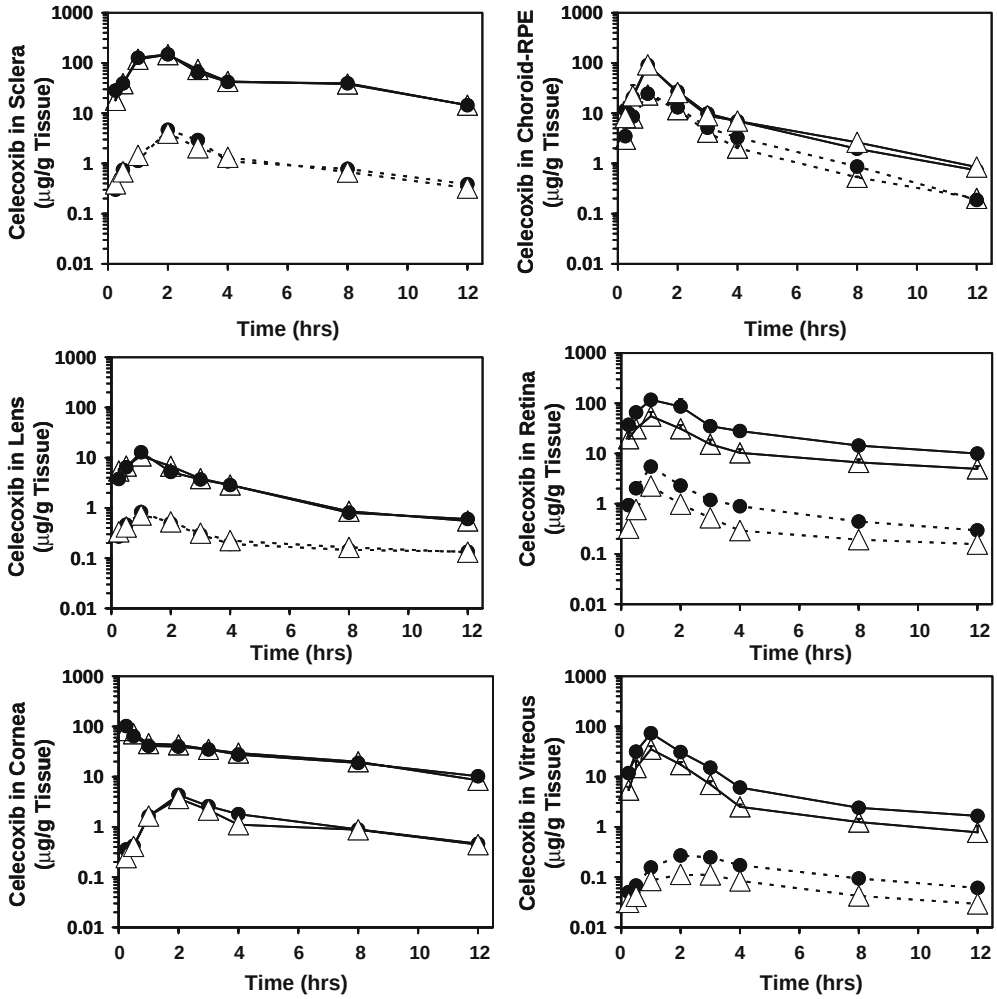

Fig. 3. Influence of diabetes on celecoxib delivery following periocular injection in (*open triangle*) control and (*closed circle*) diabetic Brown Norway rats. Key: *Continuous line* represents the ipsilateral eye and *broken line* represents the contralateral eye. Data are presented as mean±s.d. for $n=4$. The tissue concentrations for all control rats were taken from Cheruvu *et al.* (19), with permission from the Association for Research in Vision and Ophthalmology.

acetonitrile and aqueous buffer mixture (70:30 *v*/*v*). The buffer was 0.1% acetic acid in water adjusted to pH 3. The drugs were monitored at 250 nm and drug peaks were integrated using Millennium software (version 2.0). The retention times for celecoxib and budesonide were 7.1 and 5.2 min, respectively. The limit of detection of celecoxib was 1 ng in the lens and 0.5 ng in the sclera, choroid–RPE, retina, vitreous, lens and cornea.

Pharmacokinetic Parameters Estimation

The plasma and ocular tissue concentration-time profiles of celecoxib were analyzed by non-compartmental analysis using Winnonlin (Version 1.5, Pharsight). A model (200; Scientific Consulting, Inc.) with extravascular input was selected for the noncompartmental analysis and the samples were weighted uniformly. The area under the plasma/tissue concentration-time curve ($AUC_{0-\infty}$) was calculated by the log linear trapezoidal method in which the area from the last concentration point T_{last} (nanograms per milliliter for plasma or micrograms per gram for ocular tissues) to infinity was calculated as C_{last}/K, where C_{last} was the concentration at T_{last} and K (h^{-1}) was the rate constant calculated from the terminal phase. The terminal phase rate constant was obtained using data from 3 to 12 h. The units for AUC are nanograms. (hour per milliliter) and micrograms. (hour per gram) for plasma and ocular tissues, respectively. In each tissue, the maximum concentration observed (C_{max}) and the time at which C_{max} occurred (t_{max}) were determined. Also, the apparent volume of distribution (V_d/F), apparent clearance (Cl/*F*), and terminal half-life ($T_{1/2}$) were estimated. F indicates fraction absorbed. For comparison of pharmacokinetic parameters between the control and diabetic animals in albino and pigmented strains, eight random noncompartmental analyses were performed on the SD and BN rat data ($n = 4$ for each time point) and the derived parameters were compared as described under statistical analysis. The percentage of local drug delivery was determined as described previously (45).

Statistical Analysis

Data are expressed as mean ± SD. The statistical comparisons between the tissues of control and diabetic rats of both the strains were performed using non-parametric Mann–Whitney test. Comparison of FITC-dextran leakage in retina and drug concentration comparisons between different tissues were performed using an ANOVA with Tukey's post-hoc analysis. Differences were considered significant at $p < 0.05$.

RESULTS

Animal Weights and Blood Sugar Levels

Summary of body weights and blood sugar levels in control and diabetic SD and BN rats is tabulated in Table I. There is no significant difference in the average body weight and blood sugar levels between the strains.

Table IV. Influence of Diabetes on Ocular Tissue Pharmacokinetic Parameters of Celecoxib in Brown Norway Rats after Periocular Injection of Celecoxib Suspension to One Eye at a Dose of 3 mg/rat

Tissue	Group	T_{max} (h)	C_{max} (μg/g tissue)	$T_{1/2}$ (h)	$AUC_{0-\alpha}$ (μg. h/g of tissue)	Cl/*F* (g/h)	V_d/F (g tissue)
Ipsilateral eye							
Sclera	Control	1.75±0.50	175.27±16.58	4.48±0.69	899.40±111.70	4.38±0.62	27.87±3.80
	Diabetic	1.75±0.50	172.24±42.11	4.51±0.70	843.79±77.33	4.26±0.63	27.49±3.71
choroid–RPE	Control	1.00±0.00	91.81±14.62	3.69±0.25	367.12±66.06	22.25±2.44	86.7±14.71
	Diabetic	1.00±0.00	91.00±23.28	3.95±0.24	345.13±18.26	21.93±2.80	79.83±22.36
Retina	Control	1.00±0.00	55.50±9.41	6.12±0.96	476.82±57.77	14.5±0.54	128.25±21.17
	Diabetic	1.00±0.00	120.56±15.09*	5.96±1.20	1,165.58±42.10*	7.47±0.46*	48.01±9.47*
Vitreous	Control	1.00±0.00	35.26±5.15	3.23±0.57	232.94±25.11	41.85±2.99	195.75±40.577
	Diabetic	1.00±0.00	73.62±13.81*	3.35±0.46	576.63±57.26*	20.53±2.44*	101.43±5.12*
Lens	Control	1.00±0.00	10.83±1.33	8.11±0.07	175.65±32.96	84.55±6.54	379.65±26.26
	Diabetic	1.00±0.00	12.88±1.81	8.23±2.14	169.44±24.30	81.22±1.46	326.14±41.51
Cornea	Control	0.31±0.13	86.88±6.91	9.58±0.17	921.04±133.12	7.9±0.48	52.1±2.66
	Diabetic	0.79±0.21	76.23±12.10	9.42±1.06	927.16±42.78	7.47±0.84	52.18±11.48
Contralateral eye							
Sclera	Control	2.00±0.00	4.01±0.37	3.60±0.18	20.50±2.48	194.88±18.87	1,011.3±107.39
	Diabetic	2.00±0.00	4.22±1.07	3.88±0.51	19.54±1.53	205.74±21.46	1,016.60±204.51
choroid–RPE	Control	1.00±0.00	23.02±2.69	4.13±0.18	42.84±4.25	70.15±3.62	215.08±16.10
	Diabetic	1.00±0.00	24.47±5.06	3.86±0.42	41.89±3.35	69.51±9.89	230.46±59.43
Retina	Control	1.25±0.53	2.26±0.55	5.91±0.68	9.57±0.97	460.35±50.32	3,895.95±308.33
	Diabetic	1.25±0.20	5.49±0.31*	5.88±1.20	14.10±0.54*	225.48±27.26*	1,308.68±99.21*
Vitreous	Control	2.50±0.58	0.12±0.01	4.70±0.48	1.74±0.13	3,244.65±435.55	21,783.28±1,186.2
	Diabetic	2.50±0.50	0.31±0.02*	5.06±1.03	3.10±0.22*	1,502.85±90.69*	10,876.22±1,530.70*
Lens	Control	1.41±0.00	0.72±0.08	8.17±1.53	0.63±0.12	651.23±52.91	7,606.27±962.6
	Diabetic	1.50±0.87	0.75±0.14	7.13±1.97	0.62±0.07	697.73±123.46	7,988.86±1,647.89
Cornea	Control	2.00±0.00	3.69±0.18	7.64±0.39	0.70±0.22	175.1±12.93	1,167.7±83.88
	Diabetic	2.00±0.00	4.12±0.63	7.19±1.57	0.69±0.15	170.29±19.21	1,157.28±131.56

The data are expressed as mean±SD for n=4. The tissue concentrations for all control rats were taken from Cheruvu *et al.* (19), with permission from the Association for Research in Vision and Ophthalmology. C_{max}, Cl/*F*, and V_d/F values in ipsilateral eye were significantly (p=0.0001) different compared with the contralateral eye in all groups

*P<0.05 (significant difference compared to the corresponding control BN rat tissues)

Blood-Retinal Barrier Leakage

Blood-retinal barrier leakage estimated using FITC-dextran in control and diabetic SD and BN rats are shown in Fig. 1. Induction of diabetes led to significant increase in the blood-retinal barrier leakage in both the strains. In the case of SD rats, the blood-retinal barrier leakage due to diabetes (37.78 ± 7.47 μl/g per min of plasma) was ~2.5 fold higher compared to the control rats (15.68 ± 3.33 μl/g per min of plasma). For BN rats, the blood-retinal barrier leakage (56.50 ± 6.41 μl/g per min of plasma) was ~3.3 fold higher in diabetic rats compared to control rats (16.88 ± 2.39 μl/g per min of plasma).

Plasma Pharmacokinetics of Celecoxib

The plasma pharmacokinetic parameters of celecoxib following periocular administrations of celecoxib to BN and SD rats at a dose of 3 mg/rat are given in Table II. The plasma AUCs in diabetic SD (3,458 ± 542 ng.h/ml) and diabetic BN (3,317 ± 433 ng.h/ml) rats showed no significant differences compared to control SD (2,911 ± 358 ng.h/ml) and control BN (3,124 ± 435 ng.h/ml) rats. Similarly, no significant differences were seen with the other pharmacokinetic parameters, as summarized in Table II.

Ocular Tissue Pharmacokinetics of Celecoxib

Similar to our earlier findings with control SD and BN rats (19), the ocular tissue-concentration profiles in diabetic rats exhibited a rise and a fall, consistent with drug entry and elimination from the tissues. Celecoxib concentrations in all the ocular tissues for the dosed eyes (ipsilateral) were higher than the undosed (contralateral) eyes ($p = 0.0001$).

Ocular Tissue Pharmacokinetics of Celecoxib—Control *vs* Diabetic Sprague Dawley Rats

The ocular tissue concentration-time profiles of control and diabetic Sprague Dawley (SD) rats following periocular injection of celecoxib are shown in Fig. 2 and the pharmacokinetic parameters are summarized in Table III. The tissue

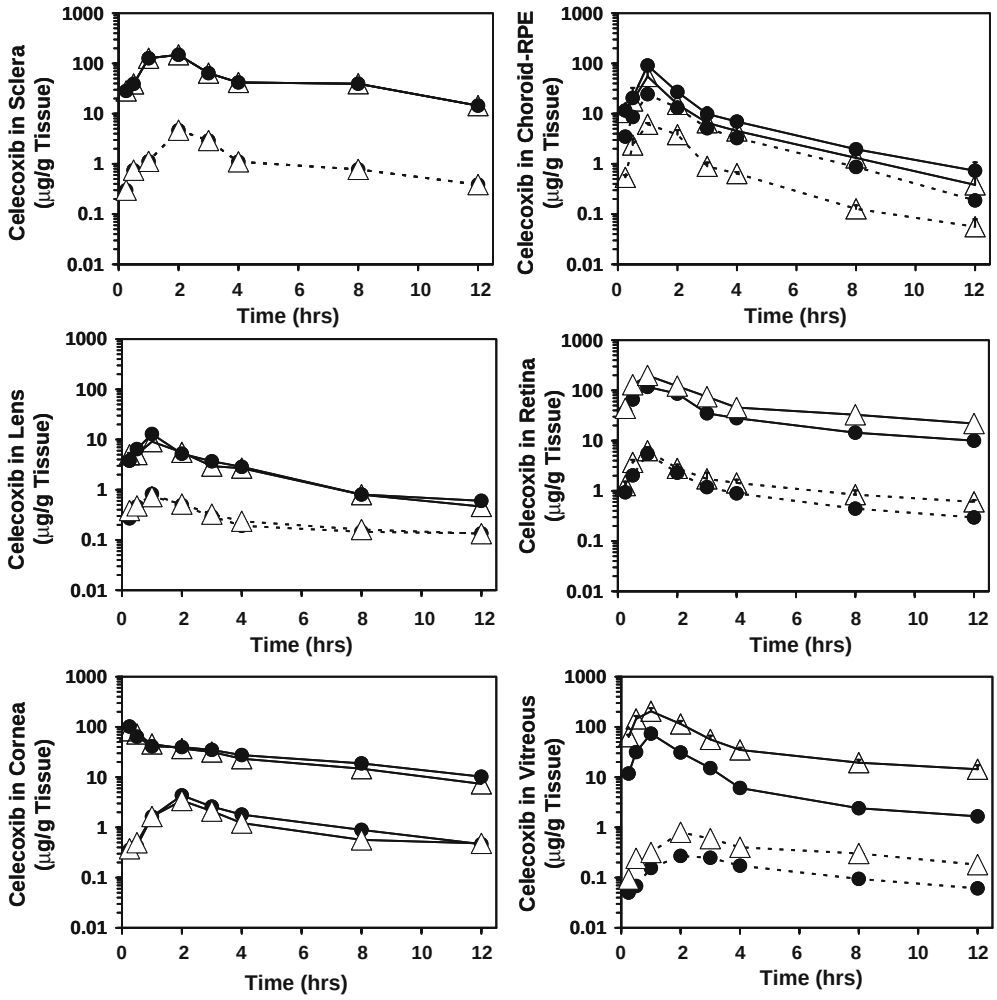

Fig. 4. Ocular tissue concentrations of celecoxib following periocular injection in diabetic Sprague Dawley (*open triangle*) and Brown Norway (*closed circle*) rats. Key: *Continuous line* represents the ipsilateral eye and *broken line* represents the contralateral eye. Data are presented as mean±s.d. for $n=4$.

AUCs were compared between control and diabetic rats for both ipsilateral and contralateral eyes in Fig. 5. The celecoxib AUC in sclera, choroid–RPE, cornea and lens between the control and diabetic albino (SD) rats were not significantly different either in the ipsilateral or in the contralateral eye. The celecoxib AUC for the ipsilateral retina (1,059.33 ± 125.78 μg.h/g) and vitreous (576.50 ± 143.89 μg.h/g) in diabetic rat were approximately 1.5-fold (p = 0.001) higher compared to the control rat retina (670.94 ± 100.69 μg.h/g) and vitreous (368.40 ± 52.14 μg.h/g). In the contralateral eyes, diabetic rat retinal (18.29 ± 1.58 μg.h/g) and vitreal (3.50 ± 0.95 μg.h/g, p = 0.04) AUC for celecoxib were about 1.3-fold (P = 0.04) higher compared to control rat retina (13.80 ± 3.92 μg.h/g) and vitreous (2.80 ± 1.13 μg.h/g).

Ocular Tissue Pharmacokinetics of Celecoxib—Control *vs* Diabetic Brown Norway rats

The ocular tissue concentration-time profiles of control and diabetic Brown Norway rats following periocular injection of celecoxib are shown in Fig. 3 and the pharmacokinetic parameters are summarized in Table IV. The tissue AUCs were compared between control and diabetic rats for both ipsilateral and contralateral eyes in Fig. 5. The celecoxib AUC in sclera, choroid–RPE, cornea and lens between the control and diabetic pigmented (BN) rats were not significantly different either in the ipsilateral or in the contralateral eye. The celecoxib AUC for the ipsilateral retina (1,165.58 ± 42.10 μg.h/g) and vitreous (576.63 ± 57.26 μg.h/g) in diabetic rat were approximately two-fold (p = 0.001) higher compared to the control rat retina (476.82 ± 7.77 μg.h/g) and vitreous (232.94 ± 25.11 μg.h/g). In the contralateral eyes, diabetic rat retinal (14.10 ± 0.54 μg.h/g) and vitreal (3.10 ± 0.22 μg.h/g, p = 0.05) AUC for celecoxib were about 1.5 and 1.8-fold (P = 0.05) higher compared to control rat retina (9.58 ± 0.77 μg.h/g) and vitreous (1.74 ± 0.13 μg.h/g), respectively.

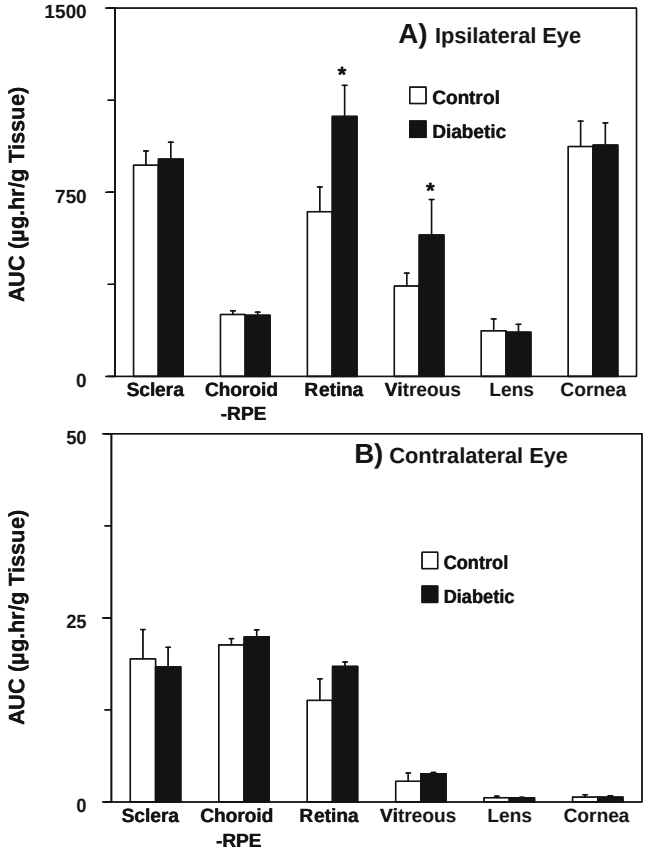

Fig. 5. Extent of celecoxib delivery ($AUC_{0-\infty}$ μg.h/g tissue) to the ocular tissues following periocular injection (3 mg to one eye) in control and diabetic Sprague Dawley (SD) rats. Data are presented as mean±s.d. for n=4. * P=0.05 compared to the control rat tissue. The tissue concentrations for all control rats were taken from Cheruvu *et al.* (19), with permission from the Association for Research in Vision and Ophthalmology.

DISCUSSION

Transscleral delivery is emerging as a safer alternative to the intravitreal mode of delivery for treating retinal disorders. In this manuscript we have investigated the effect of experimental diabetic state on the transscleral delivery of a lipophilic molecule in two rat strains. We have demonstrated that diabetes can increase the delivery of celecoxib to the retina following periocular administration probably due to the breakdown of the blood retinal barrier as a consequence of diabetes progression. There is a 1.5 and 2.4 fold increase in the retinal celecoxib AUC ratio (diabetic/control) in the SD and BN rats, respectively.

Drugs can be delivered to the retina following periocular administration by three routes: (i) passive diffusion across scleral, choroidal, and retinal pigment epithelial layers (transscleral pathway) (ii) systemic absorption of drug from the site of injection followed by its delivery through various blood vessels to the retina (46), and (iii) local haematogenous pathway (47). However, previous studies from our group (19,45) have shown that local delivery probably through the transscleral pathway accounts for >95% of the retinal celecoxib AUC in the ipsilateral (dosed) eye following periocular administration.

Increase in the AUC of celecoxib in retina as well as vitreous of diabetic rats (both SD and BN strains), could be due to the increased delivery as a result of the breakdown of the blood retinal barrier. The blood retinal barrier can breakdown at the level of the retinal endothelium (the inner blood-retinal barrier) or at the level of the retinal pigment epithelium (outer blood retinal barrier). Increased permeability at any of these anatomical locations can lead to an increase in the availability of the drugs to the retina.

There have been conflicting reports in the literature regarding the anatomical location of the breakdown of blood retinal barrier in rats (48–50). The location and extent of the barrier breakdown has been also related to the kind of tracer used for the blood retinal barrier breakdown measurements (51–56). In a comprehensive study with fluorescein as a marker, using fluorophotometry and confocal microscopy, De Camro *et al.* (51) have shown that 8 days after induction of diabetes there is a significant breakdown of the blood-retinal barrier mainly at the inner blood retinal barrier with some albeit lesser damage to the RPE. In older studies using HRP as a tracer, leakage was demonstrated at the level of both RPE and retinal vasculature (28,49). Studies using lanthanum as a tracer demonstrated leakage at the level of RPE but not

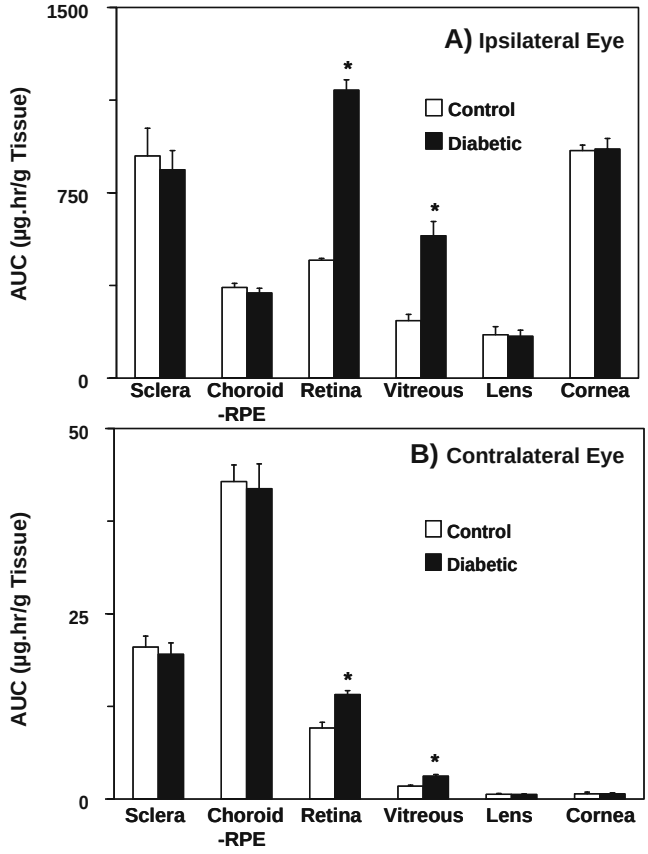

Fig. 6. Extent of celecoxib delivery ($AUC_{0-\infty}$ µg.h/g tissue) to the ocular tissues following subconjunctival injection (3 mg to one eye) in control and diabetic pigmented (BN) rats. Data are presented as mean±s.d. for n=4. * P=0.0001 compared to the control rat tissue.

retinal vasculature (57,58). Thus, the probable location of breakdown is still controversial.

We have previously evaluated the blood-retinal barrier breakdown in streptozotocin induced SD 2-month diabetic rats using a 4 kD FITC-dextran leakage assay (41). Others have used the same technique for evaluating the blood retinal barrier breakdown in normal and diabetic rats with different diabetes duration (44,57,59). In this study we used the same technique to evaluate the blood-retinal barrier breakdown in both the SD and BN rats. We observed that the blood-retinal barrier breakdown in SD rats was similar to the previous study (41), which validates the procedure. We also found that the blood retinal barrier leakage was 1.5-fold greater in diabetic BN rats as compared to diabetic SD rats. This result is in agreement with previous studies of Zhang *et al.* (29). However, the limitation of the technique is that it cannot measure the relative contribution of the outer and inner blood retinal barrier breakdown.

All the blood-retinal barrier breakdown studies evaluated the increased permeability of the markers when administered systemically. It is likely that the inner blood retinal barrier plays a more significant role in retinal delivery when the drugs are administered systemically. However, for periocular administration, the outer blood retinal barrier becomes more important than the inner blood retinal barrier as the drug has to cross the outer blood retinal barrier before gaining access to the neural retina. Even a small increase in the outer blood retinal barrier permeability can lead to a significant increase in the local delivery of the drug to the retina by the periocular route. Thus, increased celecoxib delivery to the retina and the vitreous following periocular administration might at least in part be due to the breakdown of the outer blood retinal barrier.

When we compared the retinal and vitreal celecoxib levels in the ipsilateral and contralateral eyes we found that the diabetic/control ratio of retinal celecoxib AUC was 1.6 and 1.33 in the ipsilateral and contralateral retinas of SD rats, respectively, and 2.44 and 1.50 in the ipsilateral and contralateral retinas of BN rats, respectively. Thus, the delivery increase was greater in the ipsilateral eye as compared to the contralateral eye further suggesting that the outer blood retinal barrier might also be compromised in these diabetic rats.

In some tissues, including sclera, choroid, cornea and the lens, there is no difference in celecoxib delivery in diabetic *vs.* control rats (Figs. 2, 3, 4, 5, 6, and 7). This can be explained on the basis that drug delivery to these tissues is not directly dependent on the blood retinal barrier. As planned in this study, the control and diabetic animal weights were nearly matched (Table I). Therefore, the plasma AUC as well as other plasma pharmacokinetic parameters did not differ between the control and diabetic rats in both the strains (SD and BN rats) following periocular injection of celecoxib (Table II). Thus, the observed differences in the dosed eye drug levels in the retina and the vitreous between control and diabetic rats for the two strains cannot be attributed to differences in plasma levels or pharmacokinetics, confirming a role for local factors such as the blood-retinal barrier leakage and tissue pigmentation or genetic makeup of the rats in the observed differences.

We utilized rats that were diabetic for 2 months in the current studies because we have previously observed (41) that there is a significant enhancement in the blood-retinal barrier breakdown at this time point. It is likely that the blood-retinal barrier breakdown progressively worsens with time and hence evaluation at later time points could lead to an even greater increase in the celecoxib retinal AUC. An increase of 50–140% in the retinal AUC (depending on the strain) indicates that the differences might be clinically meaningful.

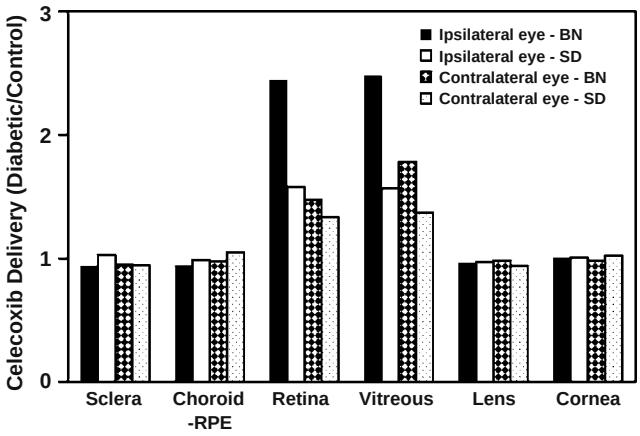

Fig. 7. Relative delivery of celecoxib in diabetic rats compared to control rats following periocular injection of celecoxib. Data are presented as the ratio of the mean AUCs or concentrations for n=4.

Whether the pathophysiology of the breakdown of the blood-retinal barrier is similar in humans and rats is still a matter of active scientific investigation; however, the breakdown of blood-retinal barrier has been demonstrated in humans using vitreous fluorophotometry and some similarities in the early pathophysiological changes in the retina as a result of diabetes have been observed in rats and humans (60–62). The results from this study indicate that the disease state has to be taken into consideration when designing therapy for retinal disorders by the periocular route. Further studies using molecules with different physicochemical properties than the one examined in this study, would be beneficial in evaluating if this observation would hold for other types of molecules including macromolecules.

In summary, the retinal and vitreal drug levels following transscleral delivery of celecoxib differ between healthy and diabetic animals. The findings of this study are clinically relevant because the breakdown of blood-retinal barrier reported in most patients during the early stages of diabetic retinopathy and the corresponding increase in retinal and vitreal concentration support the case for transscleral drug delivery.

ACKNOWLEDGEMENTS

This work was supported by NIH grants DK064172, EY013842, and EY017045 (through Emory University). We are very thankful to Leena Patel for her assistance in the preparation of this manuscript.

REFERENCES

1. S. In. Causes and prevalence of visual impairment among adults in the United States. *Am. Med. Assoc.* **122**:477–485 (2004).
2. M. V. Emerson, and A. K. Lauer. Emerging therapies for the treatment of neovascular age-related macular degeneration and diabetic macular edema. *BioDrugs*. **21**:245–257 (2007).
3. D. J. D'Amico, M. F. Goldberg, H. Hudson, J. A. Jerdan, D. S. Krueger, S. P. Luna, S. M. Robertson, S. Russell, L. Singerman, J. S. Slakter, L. Yannuzzi, and P. Zilliox. Anecortave acetate as monotherapy for treatment of subfoveal neovascularization in age-related macular degeneration: twelve-month clinical outcomes. *Ophthalmology*. **110**:2372–2383 (2003)discussion 2384–2385.
4. U. B. Kompella, N. Bandi, and S. P. Ayalasomayajula. Subconjunctival nano- and microparticles sustain retinal delivery of budesonide, a corticosteroid capable of inhibiting VEGF expression. *Invest. Ophthalmol. Vis. Sci.* **44**:1192–1201 (2003).
5. S. P. Ayalasomayajula, and U. B. Kompella. Celecoxib, a selective cyclooxygenase-2 inhibitor, inhibits retinal vascular endothelial growth factor expression and vascular leakage in a streptozotocin-induced diabetic rat model. *Eur. J Pharmacol.* **458**:283–289 (2003).
6. S. P. Ayalasomayajula, and U. B. Kompella. Subconjunctivally administered celecoxib-PLGA microparticles sustain retinal drug levels and alleviate diabetes-induced oxidative stress in a rat model. *Eur. J. Pharmacol.* **511**:191–198 (2005).
7. J. Y. Tsui, C. Dalgard, K. R. Van Quill, L. Lee, H. E. Grossniklaus, H. F. Edelhauser, and J. M. O'Brien. Subconjunctival topotecan in fibrin sealant in the treatment of transgenic murine retinoblastoma. *Invest. Ophthalmol. Vis. Sci.* **49**:490–496 (2008).
8. J. Ambati, E. S. Gragoudas, J. W. Miller, T. T. You, K. Miyamoto, F. C. Delori, and A. P. Adamis. Transscleral delivery of bioactive protein to the choroid and retina. *Invest. Ophthalmol. Vis. Sci.* **41**:1186–1191 (2000).
9. J. Ambati, and A. P. Adamis. Transscleral drug delivery to the retina and choroid. *Prog. Retin. Eye Res.* **21**:145–151 (2002).
10. I. Ahmed, and T. F. Patton. Importance of the noncorneal absorption route in topical ophthalmic drug delivery. *Invest. Ophthalmol. Vis. Sci.* **26**:584–587 (1985).
11. J. Ambati, C. S. Canakis, J. W. Miller, E. S. Gragoudas, A. Edwards, D. J. Weissgold, I. Kim, F. C. Delori, and A. P. Adamis. Diffusion of high molecular weight compounds through sclera. *Invest. Ophthalmol. Vis. Sci.* **41**:1181–1185 (2000).
12. T. W. Olsen, H. F. Edelhauser, J. I. Lim, and D. H. Geroski. Human scleral permeability. Effects of age, cryotherapy, transscleral diode laser, and surgical thinning. *Invest. Ophthalmol. Vis. Sci.* **36**:1893–1903 (1995).
13. D. E. Rudnick, J. S. Noonan, D. H. Geroski, M. R. Prausnitz, and H. F. Edelhauser. The effect of intraocular pressure on human and rabbit scleral permeability. *Invest. Ophthalmol. Vis. Sci.* **40**:3054–3058 (1999).
14. T. W. Olsen, S. Y. Aaberg, D. H. Geroski, and H. F. Edelhauser. Human sclera: thickness and surface area. *Am. J. Ophthalmol.* **125**:237–241 (1998).
15. S. B. Lee, D. H. Geroski, M. R. Prausnitz, and H. F. Edelhauser. Drug delivery through the sclera: effects of thickness, hydration, and sustained release systems. *Exp. Eye Res.* **78**:599–607 (2004).
16. M. R. Robinson, S. S. Lee, H. Kim, S. Kim, R. J. Lutz, C. Galban, P. M. Bungay, P. Yuan, N. S. Wang, J. Kim, and K. G. Csaky. A rabbit model for assessing the ocular barriers to the transscleral delivery of triamcinolone acetonide. *Exp. Eye Res.* **82**:479–487 (2006).
17. L. Pitkanen, V. P. Ranta, H. Moilanen, and A. Urtti. Permeability of retinal pigment epithelium: effects of permeant molecular weight and lipophilicity. *Invest. Ophthalmol. Vis. Sci.* **46**:641–646 (2005).
18. N. P. Cheruvu, and U. B. Kompella. Bovine and porcine transscleral solute transport: influence of lipophilicity and the Choroid–Bruch's layer. *Invest. Ophthalmol. Vis. Sci.* **47**:4513–4522 (2006).
19. N. P. Cheruvu, A. C. Amrite, and U. B. Kompella. Effect of eye pigmentation on transscleral drug delivery. *Invest. Ophthalmol. Vis. Sci.* **49**:333–341 (2008).
20. A. C. Amrite, H. F. Edelhauser, and U. B. Kompella. Modeling of corneal and retinal pharmacokinetics after periocular drug administration. *Invest. Ophthalmol. Vis. Sci.* **49**:320–332 (2008).
21. F. Ozturk, S. Kortunay, E. Kurt, S. S. Ilker, N. E. Basci, and A. Bozkurt. Penetration of topical and oral ciprofloxacin into the aqueous and vitreous humor in inflamed eyes. *Retina*. **19**:218–222 (1999).
22. F. Ozturk, S. Kortunay, E. Kurt, S. S. Ilker, U. U. Inan, N. E. Basci, A. Bozkurt, and O. Kayaalp. Effects of trauma and infection on ciprofloxacin levels in the vitreous cavity. *Retina*. **19**:127–130 (1999).
23. F. Ozturk, S. Kortunay, E. Kurt, U. U. Inan, S. S. Ilker, N. Basci, and A. Bozkurt. The effect of long-term use and inflammation on the ocular penetration of topical ofloxacin. *Curr. Eye Res.* **19**:461–464 (1999).
24. F. Ozturk, S. Kortunay, E. Kurt, U. Ubeyt Inan, S. Sami Ilker, N. E. Basci, A. Bozkurt, and S. Oguz Kayaalp. Ofloxacin levels after intravitreal injection. Effects of trauma and inflammation. *Ophthalmic. Res.* **31**:446–451 (1999).
25. F. Ozturk, E. Kurt, U. U. Inan, M. C. Kortunay, S. S. Ilker, N. E. Basci, and A. Bozkurt. Penetration of topical and oral ofloxacin into the aqueous and vitreous humor of inflamed rabbit eyes. *Int. J. Pharm.* **204**:91–95 (2000).
26. F. Ozturk, E. Kurt, U. U. Inan, S. Kortunay, S. S. Ilker, N. E. Basci, and A. Bozkurt. The effects of prolonged acute use and inflammation on the ocular penetration of topical ciprofloxacin. *Int. J. Pharm.* **204**:97–100 (2000).
27. R. Yagci, Y. Oflu, A. Dincel, E. Kaya, S. Yagci, B. Bayar, S. Duman, and A. Bozkurt. Penetration of second-, third-, and fourth-generation topical fluoroquinolone into aqueous and vitreous humour in a rabbit endophthalmitis model. *Eye*. **21**:990–994 (2007).
28. N. P. Blair, M. O. Tso, and J. T. Dodge. Pathologic studies of the blood-retinal barrier in the spontaneously diabetic BB rat. *Invest. Ophthalmol. Vis. Sci.* **25**:302–311 (1984).

29. S. X. Zhang, J. X. Ma, J. Sima, Y. Chen, M. S. Hu, A. Ottlecz, and G. N. Lambrou. Genetic difference in susceptibility to the blood-retina barrier breakdown in diabetes and oxygen-induced retinopathy. *Am. J. Pathol.* **166**:313–321 (2005).
30. A. C. Amrite, and U. B. Kompella. Celecoxib inhibits proliferation of retinal pigment epithelial and choroid-retinal endothelial cells by a cyclooxygenase-2-independent mechanism. *J. Pharmacol. Exp. Ther.* **324**:749–758 (2008).
31. L. De Schaepdrijver, P. Simoens, H. Lauwers, and J. P. De Geest. Retinal vascular patterns in domestic animals. *Res. Vet. Sci.* **47**:34–42 (1989).
32. Z. Dagher, Y. S. Park, V. Asnaghi, T. Hoehn, C. Gerhardinger, and M. Lorenzi. Studies of rat and human retinas predict a role for the polyol pathway in human diabetic retinopathy. *Diabetes*. **53**:2404–2411 (2004).
33. J. A. De Juan, F. J. Moya, A. Ripodas, R. Bernal, A. Fernandez-Cruz, and R. Fernandez-Durango. Changes in the density and localisation of endothelin receptors in the early stages of rat diabetic retinopathy and the effect of insulin treatment. *Diabetologia*. **43**:773–785 (2000).
34. A. De Roetth Jr., and F. P. Yen. Experimental diabetic retinopathy. Retinal metabolism in the alloxan diabetic rat. *Arch. Ophthalmol.* **63**:226–231 (1960).
35. E. A. Ellis, D. L. Guberski, B. Hutson, and M. B. Grant. Time course of NADH oxidase, inducible nitric oxide synthase and peroxynitrite in diabetic retinopathy in the BBZ/WOR rat. *Nitric Oxide*. **6**:295–304 (2002).
36. G. G. Quin, A. C. Len, F. A. Billson, and M. C. Gillies. Proteome map of normal rat retina and comparison with the proteome of diabetic rat retina: new insight in the pathogenesis of diabetic retinopathy. *Proteomics*. **7**:2636–2650 (2007).
37. W. G. Robison Jr. Diabetic retinopathy: galactose-fed rat model. *Invest. Ophthalmol. Vis. Sci.* **36**:(4A), 1743–1744 (1995).
38. R. Rollin, A. Mediero, A. Fernandez-Cruz, and R. Fernandez-Durango. Downregulation of the atrial natriuretic peptide/natriuretic peptide receptor-C system in the early stages of diabetic retinopathy in the rat. *Mol. Vis.* **11**:216–224 (2005).
39. E. Rungger-Brandle, and A. A. Dosso. Streptozotocin-induced diabetes—a rat model to study involvement of retinal cell types in the onset of diabetic retinopathy. *Adv. Exp. Med. Biol.* **533**:197–203 (2003).
40. Z. Zheng, H. Chen, X. Xu, C. Li, and Q. Gu. Effects of angiotensin-converting enzyme inhibitors and beta-adrenergic blockers on retinal vascular endothelial growth factor expression in rat diabetic retinopathy. *Exp. Eye Res.* **84**:745–752 (2007).
41. A. C. Amrite, S. P. Ayalasomayajula, N. P. Cheruvu, and U. B. Kompella. Single periocular injection of celecoxib-PLGA microparticles inhibits diabetes-induced elevations in retinal PGE2, VEGF, and vascular leakage. *Invest. Ophthalmol. Vis. Sci.* **47**:1149–1160 (2006).
42. S. P. Ayalasomayajula, A. C. Amrite, and U. B. Kompella. Inhibition of cyclooxygenase-2, but not cyclooxygenase-1, reduces prostaglandin E2 secretion from diabetic rat retinas. *Eur. J. Pharmacol.* **498**:275–278 (2004).
43. S. P. Ayalasomayajula, and U. B. Kompella. Induction of vascular endothelial growth factor by 4-hydroxynonenal and its prevention by glutathione precursors in retinal pigment epithelial cells. *Eur. J. Pharmacol.* **449**:213–220 (2002).
44. S. Ishida, T. Usui, K. Yamashiro, Y. Kaji, E. Ahmed, K. G. Carrasquillo, S. Amano, T. Hida, Y. Oguchi, and A. P. Adamis. VEGF164 is proinflammatory in the diabetic retina. *Invest. Ophthalmol. Vis. Sci.* **44**:2155–2162 (2003).
45. S. P. Ayalasomayajula, and U. B. Kompella. Retinal delivery of celecoxib is several-fold higher following subconjunctival administration compared to systemic administration. *Pharm. Res.* **21**:1797–1804 (2004).
46. O. Weijtens, E. J. Feron, R. C. Schoemaker, A. F. Cohen, E. G. Lentjes, F. P. Romijn, and J. C. van Meurs. High concentration of dexamethasone in aqueous and vitreous after subconjunctival injection. *Am. J. Ophthalmol.* **128**:192–197 (1999).
47. D. Ghate, W. Brooks, B. E. McCarey, and H. F. Edelhauser. Pharmacokinetics of intraocular drug delivery by periocular injections using ocular fluorophotometry. *Invest. Ophthalmol. Vis. Sci.* **48**:2230–2237 (2007).
48. T. Ishibashi, K. Tanaka, and Y. Taniguchi. Disruption of blood-retinal barrier in experimental diabetic rats: an electron microscopic study. *Exp. Eye Res.* **30**:401–410 (1980).
49. M. O. Tso, J. G. Cunha-Vaz, C. Y. Shih, and C. W. Jones. Clinicopathologic study of blood-retinal barrier in experimental diabetes mellitus. *Arch. Ophthalmol.* **98**:2032–2040 (1980).
50. I. H. Wallow. Posterior and anterior permeability defects? Morphologic observations on streptozotocin-treated rats. *Invest. Ophthalmol. Vis. Sci.* **24**:1259–1268 (1983).
51. A. Do carmo, P. Ramos, A. Reis, R. Proenca, and J. G. Cunha-vaz. Breakdown of the inner and outer blood retinal barrier in streptozotocin-induced diabetes. *Exp. Eye Res.* **67**:569–575 (1998).
52. W. M. Kirber, C. W. Nichols, P. A. Grimes, A. I. Winegrad, and A. M. Laties. A permeability defect of the retinal pigment epithelium. Occurrence in early streptozocin diabetes. *Arch. Ophthalmol.* **98**:725–728 (1980).
53. S. A. Vinores, P. A. Campochiaro, and B. P. Conway. Ultrastructural and electron-immunocytochemical characterization of cells in epiretinal membranes. *Invest. Ophthalmol. Vis. Sci.* **31**:14–28 (1990).
54. S. A. Vinores, P. A. Campochiaro, A. Lee, R. McGehee, C. Gadegbeku, and W. R. Green. Localization of blood-retinal barrier breakdown in human pathologic specimens by immunohistochemical staining for albumin. *Lab. Invest.* **62**:742–750 (1990).
55. S. A. Vinores, P. A. Campochiaro, R. McGehee, W. Orman, S. F. Hackett, and L. M. Hjelmeland. Ultrastructural and immunocytochemical changes in retinal pigment epithelium, retinal glia, and fibroblasts in vitreous culture. *Invest. Ophthalmol. Vis. Sci.* **31**:2529–2545 (1990).
56. S. A. Vinores, R. McGehee, A. Lee, C. Gadegbeku, and P. A. Campochiaro. Ultrastructural localization of blood-retinal barrier breakdown in diabetic and galactosemic rats. *J. Histochem. Cytochem.* **38**:1341–1352 (1990).
57. R. B. Caldwell, and B. J. McLaughlin. Freeze-fracture study of filipin binding in photoreceptor outer segments and pigment epithelium of dystrophic and normal retinas. *J. Comp. Neurol.* **236**:523–537 (1985).
58. R. B. Caldwell, S. M. Slapnick, and B. J. McLaughlin. Lanthanum and freeze-fracture studies of retinal pigment epithelial cell junctions in the streptozotocin diabetic rat. *Curr. Eye Res.* **4**:215–227 (1985).
59. A. W. Stitt, T. Bhaduri, C. B. T. McMullen, T. A. Gardiner, and D. B. Archer. Advanced glycation end products induce blood-retinal barrier dysfunction in normoglycemic rats. *Molec. Cell Biol. Res. Commun.* **3**:380–388 (2000).
60. J. I. Gallin, I. M. Goldstein, and R. Snyderman. *Inflammation: basic principles and clinical correlates*. Raven Press, New York, N. Y, 1992.
61. A. Garner. Histopathology of diabetic retinopathy in man. *Eye*. **7** (Pt 2):250–253 (1993).
62. K. Miyamoto, and Y. Ogura. Pathogenetic potential of leukocytes in diabetic retinopathy. *Semin. Ophthalmol.* **14**:233–239 (1999).